The Neural Cell Adhesion Molecule Is a Receptor for Rabies Virus

MARIA-ISABEL THOULOUZE,[1] MIREILLE LAFAGE,[1] MELITTA SCHACHNER,[2]
URSULA HARTMANN,[3] HAROLD CREMER,[4] AND MONIQUE LAFON[1]*

*Departement de Virologie, Institut Pasteur, Paris,[1] and IBDM/LGPD, CNRS/INSERM/Université de Méditerranée,
Campus de Luminy, Marseille,[4] France, and Zentrum für Molekulare Neurobiologie, Universität Hamburg, Hamburg,[2]
and Institut für Genetik, Heinrich-Heine-Universität, Düsseldorf,[3] Germany*

Previous reports strongly suggest that, in addition to the nicotinic acetylcholine receptor, rabies virus can use other, as-yet-unidentified receptors. We found that laboratory cell lines susceptible to rabies virus infection express the neural cell adhesion molecule (NCAM) (CD56) on their surface, whereas resistant cells do not, supporting the idea that NCAM could be a rabies virus receptor. We observed that (i) incubation with rabies virus decreases the surface expression of NCAM; (ii) treatment of susceptible cells with heparan sulfate, a ligand for NCAM, or with NCAM antibodies significantly reduces the rabies virus infection; and (iii) preincubation of rabies virus inoculum with soluble NCAM protein as a receptor decoy drastically neutralizes the capacity of rabies virus to infect susceptible cells. Moreover, we demonstrated that transfection of resistant L fibroblasts with the NCAM-encoding gene induces rabies virus susceptibility whereas absence of NCAM in the primary cortical cell cultures prepared from NCAM-deficient mice reduces the rabies virus infection and virus production. This provides evidence that NCAM is an in vitro receptor for the rabies virus. Moreover, the in vivo relevance for the use of NCAM as a receptor was demonstrated by the infection of NCAM-deficient mice, in which rabies mortality was delayed and brain invasion by rabies virus was drastically restricted. Our results showed that NCAM, which is expressed mainly in the adult nervous system, plays an important role in rabies infection. However, it cannot be excluded that receptors other than NCAM are utilized. Thus, the description of NCAM as a new rabies virus receptor would be another example of the use by viruses of more than one receptor to gain entry into the host.

The rabies virus (RV) is an enveloped bullet-shaped virus of the *Rhabdoviridae* family, genus *Lyssavirus*. The viral particle is constituted of a membrane made of host lipids and two proteins, G and M, surrounding a helical nucleocapsid (NC). The trimeric G protein is the only protein exposed on the surface of the virion. It is responsible for the attachment to the target cell by interaction with several cell membrane components. Following the attachment of G to the cell membrane, the RV enters the cell by endocytosis. Fusion of the viral membrane with endosomal membranes liberates the NC into the cytosol, where transcription and replication occur. Although RV can infect various types of cells, especially in laboratory culture conditions, its main target is the neuron. The RV binds to carbohydrates, phospholipids, and gangliosides and to protein receptors including the nicotinic acetylcholine receptor (AchR) (4). Lentz et al. observed that RV accumulates at neuromuscular junctions and colocalizes with α-bungarotoxin binding (21). They observed that preincubation of fixed chick myoblasts with α-bungarotoxin or D-turbocurarine, both of which specifically compete with acetylcholine for the AchR α subunit, and with a monoclonal antibody (MAb) against the α subunit of AchR reduced the number of myotubes infected by RV. The same group recently used a virus overlay binding assay to confirm that RV binds to the α subunit of AchR (12). These findings strongly suggest that AchR may serve as an RV receptor. However, the capacity of the RV to infect stretch proprioceptors, sensory endings, and several cell lines that do not express

AchR implies that RV can use other, as-yet-unidentified receptors (39). The identification of any such receptors would be a significant contribution to our understanding of how the RV infects cells.

The recent finding that lymphocytes support RV infection suggests that these cells also express an RV receptor (37). There is evidence that neurons and lymphocytes have common surface molecules, particularly cytokine and chemokine receptors and adhesion molecules, which have been reported to be used by viruses and parasites to infect the cells (2, 17, 28). Assuming that the RV receptor is a member of this category of molecules, we extensively surveyed the surface molecules on RV-susceptible and nonsusceptible cell lines. All RV-susceptible cell lines have the neural cell adhesion molecule (NCAM) on their surface, whereas it is not found on the surface of resistant cell lines. NCAM, also called CD56, D2CAM, Leu19, or NKH-1, is a cell adhesion glycoprotein of the immunoglobulin (Ig) superfamily which has been described for neurons, astrocytes, myoblasts, myotubes, activated T cells, and NK cells (13, 20). It is encoded by a single gene which is very well conserved among vertebrate species. Three major isoforms of NCAM, with molecular masses of 120, 140, and 180 kDa, are generated by alternative mRNA splicing (35). They all contain an almost identical ectodomain composed of five Ig-like and two type III fibronectin-like domains. The major differences among the three isoforms are in their transmembrane and cytoplasmic domains: only NCAM-120 is linked to the membrane via a phosphatidylinositol-glycan transmembrane anchor, and NCAM-140 and NCAM-180 have cytoplasmic tails of different lengths. Additional diversity among these subtypes is generated by alternative splicing of transcripts encoded by several small exons, resulting in differences in ectodomain size and glycosylation. All three forms can be posttranslationally modified by addition of polysialic acid, a carbohydrate moiety.

* Corresponding author. Mailing address: Institut Pasteur, Unité de Neurovirologie et Régénération du Système Nerveux, Groupe de Neuro-Immunologie Virale, 25, rue du Dr. Roux, 75724 Paris Cedex 15, France. Phone: 33 1 45 68 87 52. Fax: 33 1 40 61 33 12. E-mail: mlafon@pasteur.fr.

The goal of the work was to determine the role of NCAM in RV infection both in vitro and in vivo. We assayed in vitro the effect of NCAM blockage by ligands and the neutralization of virus by soluble NCAM. We also analyzed RV infection of cells transfected with genetic constructs encoding various NCAM isoforms (-140 or -180) (15). The role of NCAM in vivo was investigated by using knockout mice lacking all three isoforms of NCAM (9). We demonstrate that NCAM is a receptor for the RV. Thus, the RV can utilize at least two different receptors, AchR and NCAM, to invade the host.

MATERIALS AND METHODS

Cells and viruses. Mouse NCAM-negative L fibroblasts and stable L NCAM-negative cells expressing the full-length mouse NCAM isoform, D9 and A14 cells (15), and laboratory cell lines were grown as described in the literature. RV laboratory strain CVS (challenge virus standard) was obtained from the American Type Culture Collection, Manassas, Va. (no. vr959). Vaccinia virus was a gift from Robert Drillien. RV and vaccinia virus were propagated on BSR cells, and cell culture supernatants were used as inocula. RV was also purified from supernatants of infected cells on a sucrose gradient and concentrated as previously described (37). For ^{35}S labeling of the RV, cell culture medium was replaced 2 days after infection by methionine-free minimal essential medium (MEM) supplemented with 5 µCi of Trans^{35}S per ml for 4 days, purified on a sucrose gradient, and concentrated. Cells and viruses were mycoplasma free as determined by the plaque assay technique.

Animal model. NCAM-deficient mice were generated by gene targeting and came from Harold Cremer (9). NCAM-positive or -negative mice were tested either by allele-specific PCR analysis of genomic DNA or by immunohistochemistry with an anti-NCAM antibody (Ab) recognizing all three NCAM isoforms. Brain and cortical cell cultures from genotype NCAM$^{+/+}$ and NCAM$^{+/-}$ mice, found to express NCAM by immunohistochemistry, were recorded as wild-type phenotype, whereas material from genotype NCAM$^{-/-}$ mice, presenting a total lack of NCAM protein expression, was classified as NCAM-KO phenotype.

Antibodies (MAbs) and reagents. Texas red-conjugated streptavidin, MEM, RPMI, Ham's F-12 medium, and methionine-free MEM were obtained from Gibco BRL (Cergy-Pontoise, France). Phycoerythrin-conjugated streptavidin was from Dako (Glostrup, Denmark). Biotin-conjugated anti-mouse IgG goat Ab and the ECL kit were purchased from Amersham (Little Chalfont, Buckinghamshire, United Kingdom). Mouse MAb directed against mouse NCAM (CD56), rat MAb directed against the α6 chain of integrin (CD49f) or CD9 molecules, and a mouse polyclonal Ab directed against human CD56 were obtained from PharMingen (San Diego, Calif.). The rat H28 purified MAb (IgG2a), directed against mouse brain tissue-extracted NCAM, was a gift from Christo Goridis (16). The rat IgG2a MAb (anti-Vβ6 T-cell receptor) used as the isotype matching control was from the laboratory. Fluorescein isothiocyanate (FITC)-conjugated NC-specific rabbit Abs were purchased from Sanofi Diagnostics (Marnes la Coquette, France). Purified recombinant soluble NCAM protein, containing all five Ig domains and the two type III fibronectin-like repeats, was produced in bacteria and purified as previously described (11). Rabbit polyclonal anti-IgG3 and Trans^{35}S label were obtained from ICN Pharmaceuticals (Costa Mesa, Calif.), and mouse anti-human CD3 was obtained from Dako. DNase I; aprotinin; phenylmethylsulfonyl fluoride; laminin; heparan sulfate; and chondroitin sulfate A, B, and C were purchased from Sigma Chemical (St. Louis, Mo.). Cell Fix buffer and Cell Quest software were from Becton Dickinson and Co. (Mountain View, Calif.). Vectashield medium was from Vector Laboratories, distributed by Biosys, Compiegne, France.

NCAM modulation after virus binding. BSR or N2a (5×10^5) cells were incubated in glass tubes with either 50 µl of CVS virus (10 to 30 PFU per cell) in MEM–2.5% fetal calf serum (FCS), 50 µl of vaccinia virus inoculum, or 50 µl of MEM–2.5% FCS as a control for 30 min at 37°C. Cell suspensions were incubated for a further 30 min with 50 µl of either anti-NCAM MAb, anti-α6 chain of integrin MAb, or MEM–2.5% FCS; washed in phosphate-buffered saline (PBS)–CaMg; and incubated for 30 min at 4°C with either FITC-conjugated anti-mouse IgG Ab or anti-rat IgG Ab. Cells were then fixed in Cell Fix buffer and analyzed by flow cytometry with a FACScalibur cytofluorimeter and Cell Quest software.

Western blot. N2a, D9, A14, and control L cells were tested for NCAM by Western blotting. For each cell line tested, 20 µl of total cell extract (corresponding to 5×10^6 cells) was subjected to sodium dodecyl sulfate-polyacrylamide gel electrophoresis and transferred to nitrocellulose membranes. NCAM was revealed by incubating the membranes with the mouse anti-CD56 MAb, followed by biotinylated anti-mouse IgG Ab and horseradish peroxidase-conjugated streptavidin with the ECL kit.

Cell infection assays. RV infection was quantified by the previously described fluorescent focus assay (19). The degree of infection was expressed as percentage of infected cells per well. To analyze the effect of anti-NCAM Ab on RV infection, N2a or BSR cell monolayers in 96-well titration plates were incubated either with rabbit Ab directed against NCAM or against an irrelevant protein (IgG3) or with a rat MAb directed against NCAM (H28) or another surface

molecule (either α6 chain of integrin [CD49f] or CD9) or an irrelevant protein (anti-Vβ6 T-cell receptor) in 50 µl of MEM–2.5% FCS for 30 min at 4°C. Abs were removed before cells were infected. To determine the effect of heparan sulfate on RV infection, N2a, BSR, or L cell monolayers were treated with heparan sulfate or chondroitin sulfate A, B, or C as a control (10 µg/ml in 50 µl of MEM–2.5% FCS) for 30 min at 37°C. Glycoaminoglycans were removed before cells were infected. For all cell infection assays, serial threefold dilutions of RV were added to the cultures in the same medium and the samples were incubated for 1 h at 37°C under 5% CO_2. The medium was replaced with MEM–8% FCS, and the incubation was continued for 18 h at 37°C under 5% CO_2. Percentages of cells infected were determined for each culture condition. The percentage of inhibition of infection was calculated thus: $100 \times$ (percentage of infected cells in the control $-$ percentage of infected cells in the assay)/ (percentage of infected cells in the control). Controls were either cells treated with irrelevant Ab in the antibody competition experiments or nontreated cells in inhibition experiments with glycosaminoglycans.

Binding assay. N2a, D9, A14, or control cells (5×10^5 cells) were incubated with ^{35}S-labeled virus (15,000 cpm) in 100 µl of PBS containing 0.2% bovine serum albumin for 1 h at 4°C. Cells were then centrifuged at low speed ($600 \times$ g for 7 min) and washed twice in PBS-CaMg. Virus bound to cells was measured with a beta counter.

Virus neutralization. To analyze the effect of soluble NCAM protein on RV neutralization, BSR cells were infected with viral inoculum preincubated with soluble NCAM or with control proteins (Ig anti-human CD3 and laminin). Inocula containing 13 µg of concentrated RV or vaccinia virus (as a control) were first incubated with 0.7 to 1 µg of soluble NCAM or control proteins for 40 min at 37°C. Residual infectious RV and vaccinia virus were then quantified with BSR cell monolayers. Infection was monitored as the percentage of cells infected, and results are expressed in percentages of viral neutralization.

Infection of cortical cell cultures. The cortex was dissected out from each newborn (less than 2 days old) littermate mouse obtained from NCAM$^{+/-}$ female mice mated with NCAM$^{-/-}$ male mice. The tissues were collected individually in Ham's F-12 medium, triturated in trypsin (0.025%), and incubated for 45 min at 37°C. DNase I was added to the mixture for the last 15 min. Cortical cells were dissociated by several passages through a glass Pasteur pipette and counted. Cells were seeded on polyornithine-treated (15 µg/ml) round glass slides in 24-well tissue culture plates (2×10^6 cells/ml) in Ham's F-12 medium supplemented with 10% FCS and grown at 37°C under 7% CO_2. After 3 days, cortical cell cultures were washed and infected with CVS RV at a multiplicity of infection (MOI) of 10 in 0.2 ml of Ham's F-12 medium–10% FCS or uninfected as a control, by a 1-h contact at 37°C under 5% CO_2. Cell cultures were then washed to remove the viral inoculum and incubated at 37°C under 5% CO_2 for further analysis. Infection was monitored both as the percentage of cells infected and as virus produced and released into the culture supernatant 6 days after infection by the plaque-forming assay with CER cells as described elsewhere (19). Results are expressed in virus production per a definite number of cells in culture.

Immunocytochemistry and immunohistochemistry. Double immunostaining was performed in two steps. First, cells were surface stained with anti-NCAM MAb diluted in staining buffer (PBS containing 1% heat-inactivated FCS and 0.1% [wt/vol] sodium azide) for 30 min at 4°C, washed, and incubated with biotin-conjugated anti-mouse Ig MAb and Texas red- or phycoerythrin-conjugated streptavidin under the same conditions. Intracellular NC was then immunodetected by further incubation with FITC-conjugated NC-specific Ab diluted in permeabilization solution (PBS containing 0.2% Triton X-100 and 3% heat-inactivated FCS) for 30 min and then by washing the cells in PBS. The cells were then examined with a UV microscope (Carl Zeiss, Inc., Thornwood, N.Y.) or by cytofluorimetry. Adult wild-type and NCAM-deficient 6- to 8-week-old mice were inoculated with 10^7 PFU of the CVS strain in the right and left masseter muscles. Mice were sacrificed. After perfusion with 4% paraformaldehyde in PBS, brains were removed and fixed by immersion in the same fixative overnight and then in 15% sucrose in PBS. Twenty-micrometer-thick sections were cut on a cryostat and placed in blocking buffer (PBS containing 10% heat-inactivated FCS) for 1 h at 37°C. Floating sections were treated for 2 h at 37°C with FITC-conjugated NC-specific Ab, diluted in PBS containing 2% FCS and 0.3% (vol/vol) Triton X-100, and then rinsed three times with PBS. The sections were then placed onto slides, dried at room temperature, coverslipped in Vectashield medium, and examined under a UV microscope.

Quantification of RV infection of the brain by ELISA. Unfixed brains from RV-infected mice were removed 6 days postinfection, washed in PBS, and separated into three parts: cortex, cerebellum plus brain stem, and diencephalon. Tissues were then dissociated into RPMI medium containing 2% bovine serum albumin, aprotinin, and phenylmethylsulfonyl fluoride and frozen until the analysis. RV N protein was assayed by a capture enzyme-linked immunosorbent assay (ELISA) as previously described (26). Results are expressed in picograms of N protein per milliliter with a standard N protein (a gift from André Aubert) preparation as reference.

NCAM-deficient and wild-type mouse mortality. Six- to eight-week-old female wild-type and NCAM-deficient mice were inoculated intramuscularly in the thigh of both hind legs with the CVS strain of RV (10^6 PFU per mouse). Deaths were scored daily for 15 days postinfection.

TABLE 1. Infection of cell lines

Cell line	Origin	RV susceptibility[a]	Presence of NCAM on surface[b]
IMR-32	Human neuroblastoma	100	+++
N2a C1300	Mouse neuroblastoma	100	+++
Vero	African green monkey kidney cells	100	+++
CER	Chicken embryo related (or hamster)	80–100	++
BSR and BHK-21	Hamster kidney cells	80–100	++
NIH 3T3	Embryonic mouse fibroblast	80–100	++
CHO-K1	Hamster ovary	80–100	+++
WEHI 7.1	Mouse lymphoma	100	+++
L-929 and L cells	Mouse fibroblast	1–5	−
YAC-1	Mouse lymphoma	1–5	−
HeLa	Human epithelioid carcinoma, cervix	10	−
HEp-2	Human epidermoid carcinoma, larynx	10	−
MRC5	Human lung	30	± (faint fluorescence in only a few cells)
PC12	Rat adrenal pheochromocytoma	8	−
NGF-treated PC12	Rat adrenal pheochromocytoma	28	+[c]

[a] Measured as the percentage of cells infected 24 h after initial contact with virus. Permeabilized cells were stained with anti-rabies NC rabbit Ab conjugated with FITC.

[b] Surface NCAM was revealed with either anti-human CD56 Ab or an anti-mouse CD56 MAb depending on the origin of the cells. Anti-mouse and anti-human CD56 Abs cross-react with hamster and rat and simian NCAM, respectively.

[c] Forty-three percent.

Statistical analysis. Differences between NCAM-deficient and wild-type mouse groups were analyzed by appropriate frequency analysis including Fisher's exact test and Student's t test.

RESULTS

RV infects NCAM-positive cells. Cell lines of human-simian, chicken, or rodent (mouse, rat, and hamster) origin were tested for their susceptibility to the rabies CVS strain at an MOI of 1. Percentages of cells infected 24 h after initial contact were recorded (Table 1). The cell lines could be classified into two groups. The first group consisted of susceptible cell lines in which infection spread rapidly (80 to 100% of the cell population infected within 24 h). A second group was composed of RV-resistant cell lines: less than 10% of the total cells infected after 24 h. The human MRC5 cell line was intermediate, with 30% of cells infected. We tested whether different susceptibilities corresponded to differences in the viral binding. Aliquots (5×10^5 N2a and L cells) were incubated for 1 h at 4°C with 15,000 cpm of ^{35}S metabolically labeled RV, and 2,968 ± 269 cpm bound to N2a whereas only 1,536 ± 241 cpm bound to L cells (significant at $P = 0.003$) (data not shown).

The cell lines were tested for surface expression of NCAM by an anti-NCAM MAb staining technique. NCAM was found on the surface of the susceptible cell lines (IMR-32, N2a, Vero, BSR, CER, CHO-K1, WEHI 7.1, NIH 3T3, and MRC5 cells) but not on that of the resistant cell lines (L cells, L-929, YAC-1, HeLa, HEp-2, and undifferentiated PC12) (Table 1). Note that only 20% of the MRC5 cells, a line poorly susceptible to infection (30%) were stained, suggesting that rabies susceptibility correlated with the level of NCAM expression in the cell population. To assess this possibility, we used nerve growth factor (NGF) supplementation, a treatment which upregulates NCAM production in PC12 cell cultures (10). PC12 cells were supplemented with NGF (50 ng/ml for 48 h). NCAM was consequently produced in 43% of cells in the culture. This was paralleled by increased susceptibility to RV (28% of NGF-treated PC12 cells were infected compared to 8% of the undifferentiated PC12 cells). Thus, the susceptibility of cultivated cell lines to RV correlates with NCAM expression.

In the experiments described below, we used three cell types as model systems to study the role of NCAM in RV infection: N2a, BSR, and L cells. The RV-susceptible, mouse neuroblas-toma N2a line expresses both NCAM and nicotinic AchR, the baby hamster kidney BSR cells express NCAM only, and the non-RV-susceptible, mouse fibroblast L cells do not produce either NCAM or AchR.

RV decreases surface expression of NCAM. We analyzed the effect of an incubation with RV on the expression of NCAM on the cell surface of N2a and BSR cells. Cells were incubated at 37°C for 30 min with a series of doses of RV (10 and 30 infectious particles per cell) or PBS (mock treated). NCAM surface expression was compared in the three populations by cytofluorimetry with an anti-NCAM Ab (Fig. 1). Exposure to the virus decreased the intensity of fluorescence, and the effect was dose dependent: 61.4 mean fluorescence in mock-treated BSR cells, 55.5 in BSR cells treated with 10 PFU per cell, and 33.3 in BSR cells treated with 30 PFU per cell. The findings for NCAM fluorescence in N2a cells were similar (Fig. 1C). This decrease in NCAM fluorescence intensity was not observed if the virus and BSR or N2a cells were incubated at 4°C (data not shown), a temperature that does not allow internalization despite virus attachment to the cells. The fact that this phenomenon was observed only at a physiological temperature is consistent with the binding of virus to the cell surface triggering internalization of NCAM surface molecules.

We analyzed the effect of vaccinia virus on the surface NCAM on BSR cells, which are also susceptible to this virus (Fig. 1B). Incubation of BSR cells with vaccinia virus does not affect surface NCAM, indicating that the loss of surface NCAM is RV specific. We then analyzed the effect of RV on the surface behavior of other integral proteins of the N2a cell membrane, the α6 chain of integrin and CD9. The treatment of N2a cells with RV in the conditions that resulted in the loss of NCAM (Fig. 1C) did not modify the amount of α6 chain of integrin molecules on the surface (Fig. 1D). Similarly, RV did not affect the expression of CD9 molecules on the surface of BSR cells (data not shown).

These observations indicate that treatment with RV does not trigger a general perturbation of the membrane structure and suggest that RV specifically modulates the surface expression of NCAM. Since RV enters cells by an adsorptive endocytosis pathway, the partial disappearance of NCAM from the cell surface may well be the consequence of the internalization of NCAM-virus complexes in endocytosis vesicles.
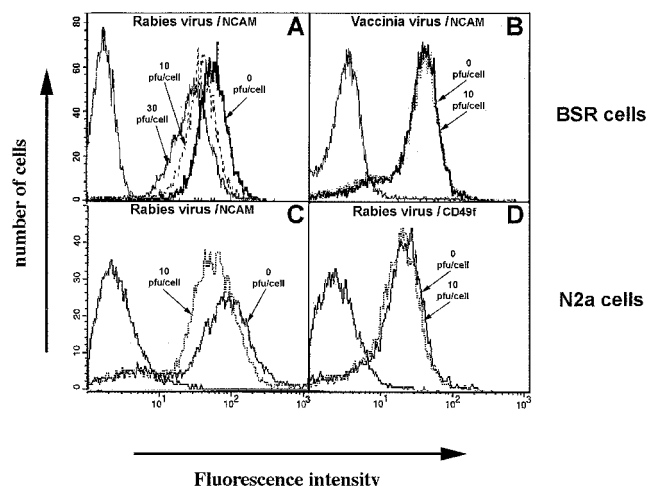
FIG. 1. RV modulates NCAM expression on the cell surface. Modulation by RV of the amount of NCAM on the cell surface of BSR (A and B) and N2a (C and D) cells was analyzed by cytofluorimetry. BSR cells were either mock treated (incubation with medium alone) (solid bold line) or treated with 10 (dashed line) or 30 (solid line) PFU of RV per cell (A) or with 10 PFU of vaccinia virus per cell (dotted line) as control virus (B). The samples were then incubated with anti-NCAM MAb or culture medium (peak on the extreme left) followed by FITC-conjugated anti-mouse IgG. The specificity of NCAM modulation by RV was tested by using N2a cells, which express both NCAM and α6 chain of integrin (C and D). N2a cells were either mock treated (solid line) or treated (dotted line) with 10 PFU of RV per cell and then anti-NCAM MAb (C) or an anti-α6 chain of integrin MAb (D) or culture medium (left peak in diagrams) followed by FITC-conjugated anti-mouse IgG Ab. Values are representative of five independent experiments.
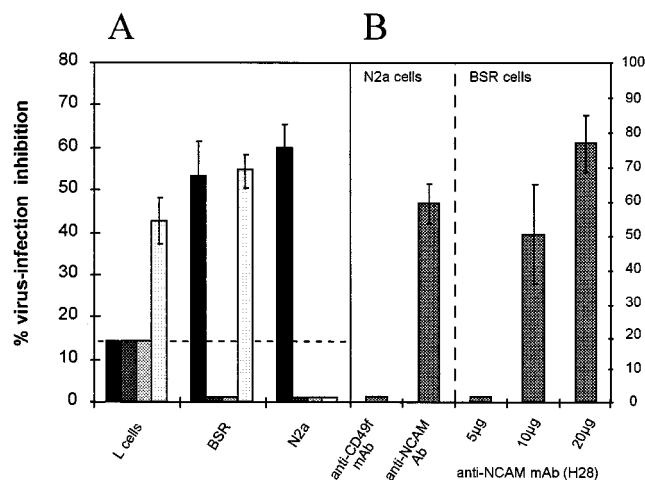

FIG. 2. Glycosaminoglycans (A) and anti-NCAM Abs (B) inhibit RV infection. (A) NCAM-negative (L cells) and NCAM-positive (BSR and N2a) cell monolayers were incubated for 30 min at 37°C with 10 μg of heparan sulfate (black bars) or chondroitin sulfate A (dark gray bars), B (light gray bars), or C (white bars) per ml. (B) NCAM-positive (N2a) cell monolayers were incubated for 30 min at 4°C with 5 μg of MAb directed against the α6 chain of integrin (MAb CD49f) per ml, rabbit serum directed against recombinant soluble NCAM protein, or their respective controls. NCAM-positive (BSR) cell monolayers were incubated with increasing doses of anti-NCAM (H28) MAb (5 to 20 μg/ml) or isotype control MAb. After ligand or Ab treatment, cells were inoculated with RV and infection was estimated as the percentage of NC-positive cells 18 h postinfection. The percentage of inhibition of infection was calculated thus: 100 × (percentage of infected cells in the control − percentage of infected cells in the assay)/(percentage of infected cells in the control). Values are the means of three independent experiments ± standard deviations.

Heparan sulfate and Ab directed against NCAM inhibit RV infection. We analyzed whether blocking NCAM decreased cell susceptibility to RV infection. We first tested the effect of heparan sulfate, a physiologically relevant natural ligand of NCAM (7). NCAM-positive cells (BSR or N2a cells) and negative cells (L cells) were either mock treated (PBS), or treated with heparan sulfate or with chondroitin sulfate A, B, or C. Chondroitin sulfate A, B, and C were used as controls for nonspecific inhibition resulting from the charge characteristics of the glycosaminoglycan. At a nontoxic concentration (10 μg/ml), heparan sulfate inhibited RV infection by up to 60% in N2a cells and 55% in BSR cells but only by 13% in L cells (Fig. 2A). Unexpectedly, unlike chondroitin sulfate A and B, chondroitin sulfate C strongly inhibited RV infection in BSR cells (53%) and in NCAM-negative L cells (43%). To our knowledge, chondroitin sulfate C has not been reported to be an NCAM ligand and the mechanism of the antagonist effect has not been described yet.

To confirm the role of NCAM in virus entry, we treated N2a and BSR cells with polyclonal Ab directed against NCAM or with control Ab before infection. NCAM-specific Abs were raised against a native NCAM preparation (1). NCAM Ab pretreatment inhibited infection of N2a cells by 60% (Fig. 2B, left part) as well as that of BSR cells (data not shown), whereas rabbit preimmune Ab or irrelevant Ab had no effect. Similar findings were obtained when BSR cells were treated with a rat MAb directed against NCAM (H28 MAb). As shown in the right part of Fig. 2B, pretreatment of BSR cells with H28 MAb strongly inhibited RV infection (49% inhibition of infection with 10 μg of H28 and up to 76% with 20 μg of H28 MAb).

A pretreatment of N2a cells with an anti-CD49f MAb directed against the α6 chain of integrin, or with an isotype control MAb, did not modify the RV N2a susceptibility. This indicates that the NCAM Ab-mediated inhibition was NCAM specific.

These results indicate that occupancy of cell surface NCAM by Ab or heparan sulfate can block RV infection of cells expressing NCAM. This strongly supports the hypothesis that NCAM is a receptor for RV.

Soluble NCAM neutralizes RV infection. Our next approach was to test whether treatment of RV with a soluble NCAM preparation neutralized the virus particles. Viral inocula were incubated with a series of doses of soluble NCAM (0.7 to 1 μg) or with medium alone and assayed for their residual capacity to infect BSR cells (Fig. 3). Pretreatment of RV with concentrations of NCAM dose dependently reduced (up to 100%) the capacity of RV to infect cells (Fig. 3) and reduced virus production by infected cultures by a factor of 1,000-fold (3-log reduction in the virus titers) (data not shown). The NCAM dose-effect curve was not linear (Fig. 3), indicating a two-step reaction, consistent with the fact that G molecules are associated in trimers on the surface of RV. In contrast, NCAM (0.75 or 1 μg) pretreatment of vaccinia virus did not decrease its capacity to infect BSR cells (right part of Fig. 3), indicating that NCAM treatment was not toxic either for the cells or for the viral inoculum. Neither laminin (even at 100 μg) a component of the basement membrane, nor an irrelevant protein had any effect (extreme left of Fig. 3), indicating that the neutralization effect was NCAM specific.

These observations suggest that RV G, the virion surface protein responsible for the attachment of virus particle to cells, has a fixation site for NCAM and that occupancy of this site abolishes further binding to RV receptors on the target cell.

Transfection of resistant L cells with *NCAM* cDNA induces RV susceptibility. We tested whether transfection of resistant cells with *NCAM* cDNA resulted in susceptibility to RV. Four different cell lines were used: L cells transfected with NCAM genes coding for NCAM-180 (D9 cells) or -140 (cell line A14), N2a cells that produce all three isoforms (180, 140, and 120), and negative RV-resistant L cells (see Western blotting anal-
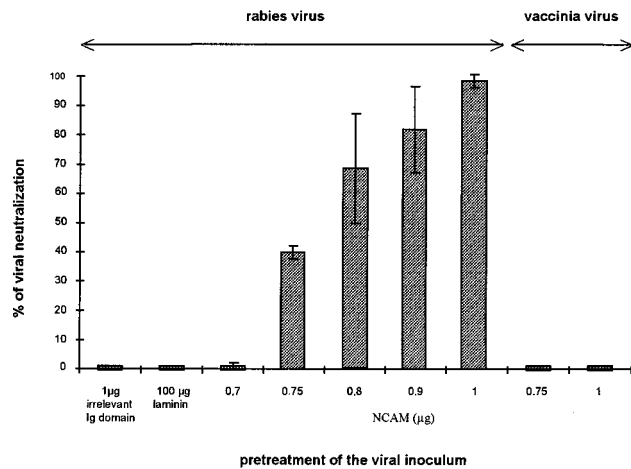
FIG. 3. Soluble recombinant NCAM protein neutralizes RV infection. RV and vaccinia virus inocula were incubated with 0.7 to 1 μg of soluble NCAM or with control proteins (irrelevant Ig domain and laminin) for 40 min at 37°C. The effect of the different treatments was estimated by measuring the residual infectious virus expressed as a percentage of BSR cells infected after 18 h of culture (left part for RV and right part for vaccinia virus). Values are the means of four separate experiments ± standard deviations.

ysis in Fig. 4). Cytofluorimetric analysis of NCAM expression in the four types of cells revealed differences in intensity and distribution of fluorescence. NCAM was detected on the surface of 79% of N2a, 89% of D9, and only 55% of A14 cells (Fig. 4). NCAM surface fluorescence intensity was weaker on NCAM-transfected cells (mean fluorescence of 62.9 and 34.7 for D9 and A14 cells, respectively) than on N2a cells (mean of 142). Thus, unlike N2a cultures in which the majority of cells were brightly NCAM fluorescent (36% of the population had a fluorescence index higher than 141), strongly positive NCAM cells constituted only a small fraction of transfected cell populations (8.2 and 4% of cells in lines D9 and A14, respectively, had a fluorescence index higher than 141).

The susceptibility of the transfected cells to RV infection was compared to those of nontransfected control L and N2a cells by immunofluorescence analysis (microscopy and cyto-

fluorimetry [Fig. 5A and B]). RV antigen NC could not be detected, 18 h after infection, in the negative control cells. In contrast, transfection of NCAM-140 or -180 (A14 cells in Fig. 5A and D9 cells in Fig. 5B) conferred susceptibility to RV infection. RV in nontransfected L cells and NCAM-transfected A14 and D9 cells (Fig. 5C) was comparatively titrated. The percentages of infection at an MOI of 1 were 15% in L cells, 40% in A14 cells, and 48% in D9 cells. Moreover, the virus production was higher in transfected cells (6.5-fold in D9 cells and 5.8-fold in A14 cells) than in the nontransfected L cell control (1×10^6 PFU/ml for L cells, 7.1×10^6 PFU/ml for D9 cells, and 6.4×10^6 PFU/ml for A14 cells).

The characteristics of the transfected susceptible cells were investigated by cytofluorimetric analysis with double staining for virus and NCAM (Fig. 5B). A large majority of the infected cells were those producing NCAM: 82% of infected D9 cells and 71.5% of infected A14 cells expressed NCAM. In addition, brightly NCAM-positive cells were the preferential targets for RV infection (left panel of Fig. 5B; infected cells are concentrated in the upper right quadrant, above the dashed line). This feature is shared with N2a cells. Brightly NCAM fluorescent cells were the preferential targets for RV (middle panel of Fig. 5B, right upper quarter) whereas a clearly distinguishable population of cells characterized by weak NCAM fluorescence (bottom of the left quarter) was poorly infected. In the cell population above the dashed line, which represents brightly NCAM positive cells, 31% of the cells are infected. In contrast, in the population under the dashed line, which corresponds to cells expressing low levels of NCAM, only 3.2% of cells are infected. This 10-fold enrichment in RV susceptibility demonstrates that a high level of NCAM-180 expression is an important factor for RV infection.

To elucidate further the role of NCAM expression in susceptibility to RV, experiments involving blocking RV infection with heparan sulfate and anti-NCAM Ab were performed. Heparan sulfate treatment inhibited 37.5 and 33.3% of infection in A14 and D9 cells, respectively (Fig. 5D), confirming that the acquired susceptibility of the transfected cells was a result of the expression of NCAM and not of the transfection manipulation.

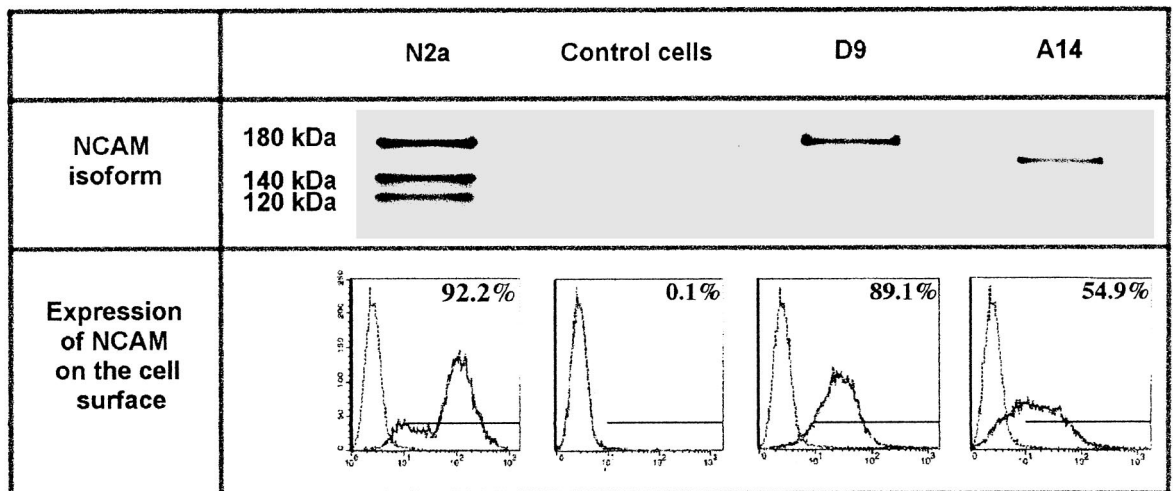Thus, transfection with *NCAM* cDNA partially restores sus-

FIG. 4. Characteristics of NCAM-transfected cells. Expression of NCAM was analyzed by Western blotting and cytofluorimetry in N2a, NCAM-negative L cells transfected with either the plasmid (control cells) or NCAM-180 (D9 cells) or NCAM-140 (A14 cells) isoform cDNA, with a MAb directed against an epitope common to the three NCAM isoforms. The solid line indicates the fluorescence profile obtained with NCAM MAb. The left peak represents FITC-conjugated secondary Ab binding. Bars and numbers represent the gated regions and percentages of cells expressing NCAM, respectively.
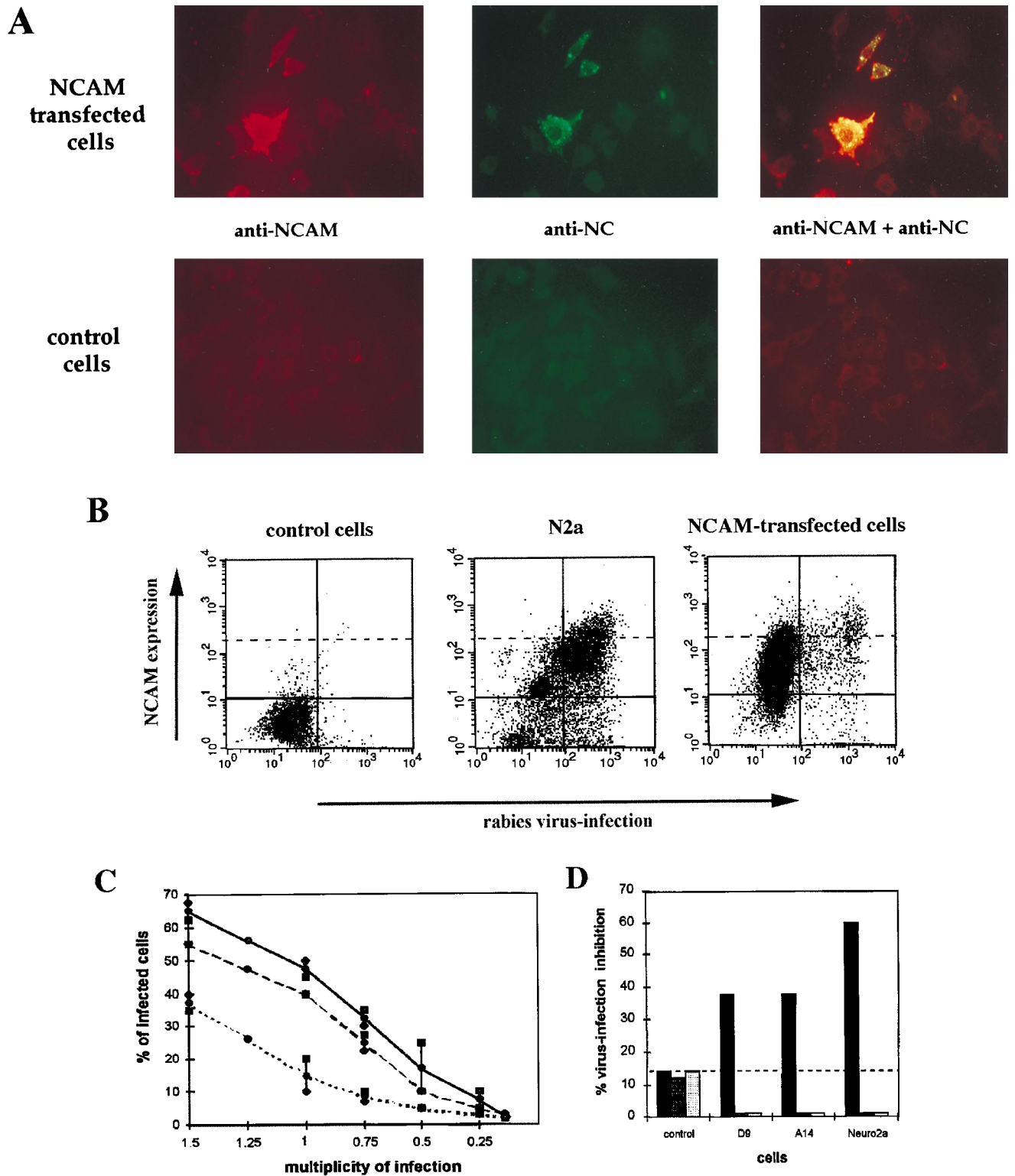
FIG. 5. RV susceptibility of transfected NCAM cells. (A and B) Two-day cultures of RV-infected N2a, NCAM-transfected (D9 and A14), and NCAM-negative (control) cells were double stained for NCAM (red) and viral NC (green) and examined by microscopy (A) or analyzed by flow cytometry (B). RV-infected NCAM-positive cells appear as yellow-stained cells in the leftmost A panels and are located in the upper right quadrant in the B panels. (C) RV susceptibility of D9 (dashed curve), A14 (solid black curve), and control (dotted curve) cells was assessed by infection with RV (MOI of 1.5 to 0.25). Results are expressed as the percentages of cells infected 48 h after infection. (D) Inhibition of RV infection of control, D9, A14, and N2a cells by heparan sulfate and chondroitin sulfate A and B (left, middle, and right bars in each set, respectively).
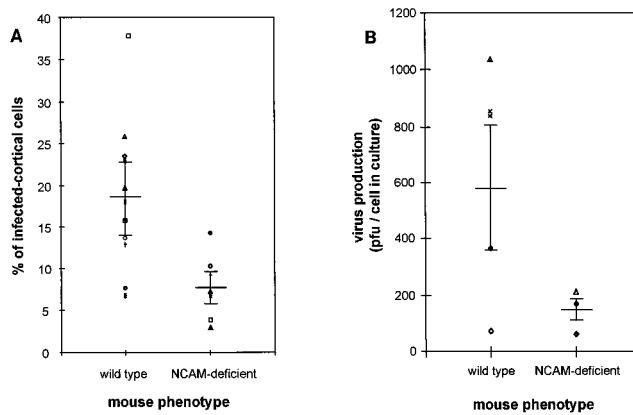
FIG. 6. RV infection of primary cortical cultures from NCAM-deficient and wild-type mice. Three-day cortical cell cultures prepared from postnatal wild-type or NCAM-deficient mice were infected with CVS at an MOI of 10 and cultivated for 3 more days. Percentages of infected cells (A) and virus production per cell in culture (B) were determined for 11 NCAM-positive and 7 NCAM-negative cortical cell cultures. NCAM-positive and NCAM-negative cortical cell cultures were tested for NCAM expression by allele-specific PCR analysis and by immunocytochemistry with an anti-NCAM MAb. Horizontal bars indicate the mean values for infection and virus production per a definite number of cells in culture ± standard deviations.

ceptibility to RV, and NCAM-transfected cells appear to become preferential targets once they express a certain amount of NCAM on their surface. These results support the previous observation that RV susceptibility correlates with NCAM expression (Table 1) and strongly suggest that there is a minimum density of NCAM which allows virus infection.

The absence of NCAM reduces the susceptibility of primary cortex cultures to RV. Day 3 primary cortex cultures were prepared from individual early postnatal wild-type and NCAM-deficient littermate mice (newborn to 2 days old). After 3 days of maintenance in vitro, they were assayed for their susceptibility to CVS infection at an MOI of 10. RV infection was evaluated by (i) the percentage of RV NC-positive cells in each culture 4 days after infection and (ii) the virus produced and released into day 7 cortex culture supernatants. The NCAM phenotype of each cortex culture was determined by testing for the presence or absence of NCAM on the surface of cortex cells with an anti-NCAM MAb and by allele-specific PCR analysis of DNA extracts from the tail of the each donor animal. The percentage of infected cortical cells was recorded for each phenotype (Fig. 6A). Cultures from wild-type cortex were significantly more infected by RV than were the NCAM-deficient cultures: the mean percentage of infected cells in the 11 wild-type cultures was 18.6 ± 8.9 compared to 7.8 ± 3.9 in the 7 NCAM-deficient cultures (significant at $P < 0.005$). Similarly, the wild-type cultures produced more virus than did NCAM-deficient cultures (582.0 ± 219 virions per cell of the wild-type culture and 147.6 ± 44.3 infectious virions per cell of NCAM-deficient cultures) (Fig. 6B).

These data demonstrate that the absence of NCAM significantly reduces the susceptibility of cortical cells to RV infection, bringing evidence that NCAM is used by RV as a receptor in the nervous system.

RV invasion is restricted in NCAM-deficient mouse brain. Progression of RV infection was monitored by immunohistochemistry on sagittal sections of brain 6 days after RV (CVS) injection into the right masseter of wild-type and NCAM-deficient mice. Although some brain structures, such as hippocampus and cerebellar Purkinje cells, were equally positive for rabies NC antigen in both groups of mice, the virus was less

extensively distributed in the brains of NCAM-deficient mice. In particular, the cortex sections were only faintly and scarcely fluorescent in NCAM-deficient mice whereas they were strongly positive in wild-type mice (Fig. 7A). The amounts of RV NC that accumulated in three different parts of the brain were compared in wild-type and NCAM-deficient mice. Nervous tissue suspensions of three parts of the brain (cerebellum plus brain stem, diencephalon, and cortex) were assayed for N protein antigen by ELISA (Fig. 7B). The suspension of cerebellum plus brain stem from NCAM-deficient mice contained fourfold-less N protein than did the wild-type cerebellum (514 ng/ml versus 2,310 ng of N protein per ml of nervous tissue suspension). Diencephalon and cortex from NCAM-deficient mice contained 16-fold less rabies antigen than those of wild-type mice (14 ng/ml versus 234 ng of N protein/ml of nervous tissue [$P < 0.005$]). These measures indicate that, after injection into the masseter muscles, the RV invades brains of NCAM-deficient mice much less efficiently than those of wild-type mice and that progression of infection is severely impaired after infection of the cerebellum and brain stem.

RV mortality is delayed in NCAM-deficient mice. We investigated whether the absence of NCAM interfered with RV infection in vivo. Adult wild-type and NCAM-deficient mice were injected with rabies CVS in the muscle of both hind legs, and the kinetics of RV-induced mortality were monitored. Nine days after inoculation, 50% of the wild-type mice were dead, whereas all the NCAM-deficient mice have survived. In the NCAM-deficient group, 50% mortality was reached only at 13 days postinjection. The mean length of survival was 13.6 days for NCAM-deficient mice and 10 days for wild-type mice (Fig. 7C). This 4-day delay in NCAM-deficient mice is consistent with the restricted viral invasion of the brain reported in Fig. 7A and B. This suggests that the absence of NCAM limits the virus progression in vivo and delays, but does not prevent, the rabies death.

DISCUSSION

We report strong evidence that NCAM expression plays an important role in cell susceptibility to RV both in vitro and in vivo. We show that (i) transfection of NCAM-negative cells (L cells) with the *NCAM* gene significantly enhances susceptibility to RV, (ii) specific blocking (antibody or natural ligand) or removal (primary cortical cell cultures prepared from NCAM-deficient mice) of NCAM drastically reduces cell susceptibility to RV, and (iii) preincubation with soluble NCAM protein as a decoy substantially decreases the capacity of RV to infect cells. We demonstrated that NCAM is a receptor for RV in vitro. The marked differences in the infection pathways and the slower progression of the disease in NCAM-deficient mice were consistent with these in vitro results and indicate that NCAM plays a significant role in vivo.

NCAM appears early in the development of all germ layer tissues. In later histogenesis, this molecule is mainly associated with muscle formation and the development of the nervous system. During the perinatal period, NCAM-positive cells include neurons and glial, skeletal, cardiac, and kidney cells as well as muscle fibers (31). The tissue distribution of NCAM is more limited in the adult: NCAM persists in most neurons and astrocytes in the central nervous system and on neural cell bodies, their nonmyelinated axons, and nonmyelinating Schwann cells in the peripheral nervous system (27). NCAM-140 is also found in adult hematopoietic tissues, where it is known as the human leukocyte differentiation antigen, CD56 (Leu19/NKH-1). CD56 is predominantly expressed on natural killer cells, in peripheral blood T lymphocytes, and in immature bone marrow cells (20). RV susceptibility of the laboratory cell lines
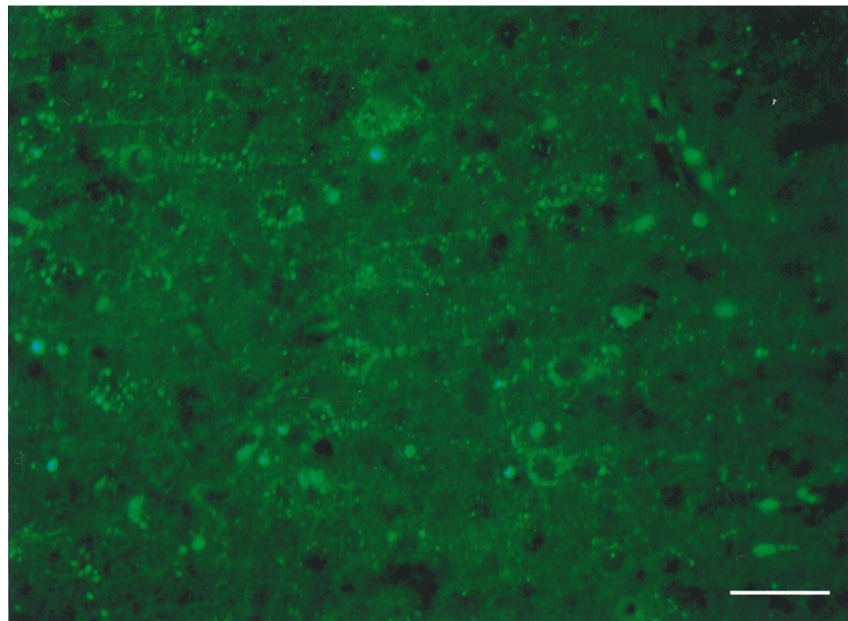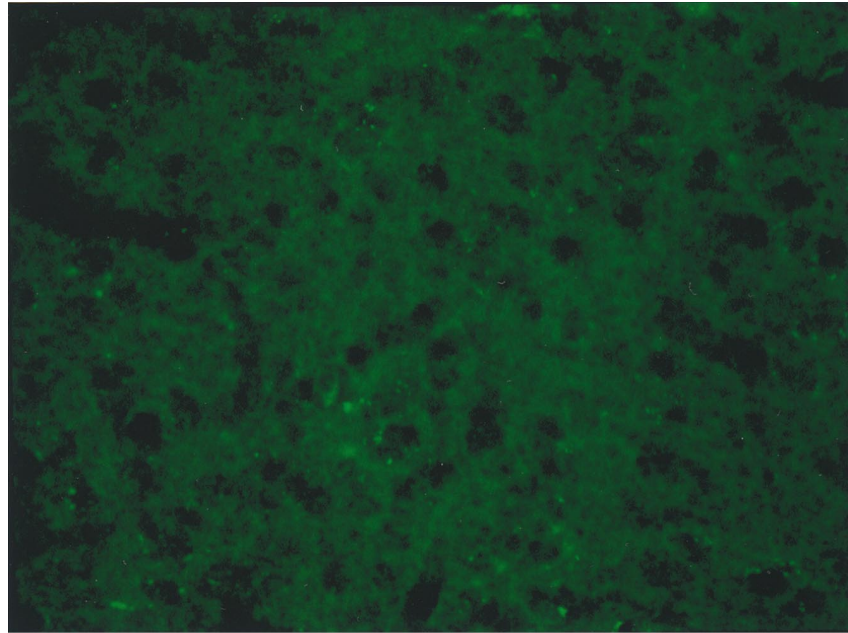
FIG. 7. RV infection and mortality in NCAM-deficient mice. (A and B) RV infection in the brains of wild-type and NCAM-deficient mice, 6 days after inoculation of the masseter muscle, was assessed by detecting RV NC by immunofluorescence (A) and N protein by immunocapture ELISA (B). (A) RV infection in cortex sagittal slices of NCAM-deficient (top) and wild-type (bottom) mice with FITC-conjugated anti-NC Ab. Bars represent 5 μm. (B) Production of RV N protein in three parts of the brain, cerebellum plus brain stem, diencephalon, and cortex, of wild-type (black bars) and NCAM-deficient (gray bars) mice. Numbers represent the N protein concentrations (picograms per milliliter) of tissue suspension. (C) Day of death according to the phenotype of mice. The mean day of death was 10.2 for the wild-type group and 13.6 for the NCAM-deficient group. Each group included eight animals. The difference was significant ($P = 0.002$).

investigated was entirely consistent with the expression of NCAM in these tissues and developmental stages. Embryos of chicken or duck origin and suckling mouse brains have been used for decades as tissues for the production of RV vaccine. Adaptation of wild strains of RV to N2a cells and to suckling mouse brain is also very efficient. Similarly, RV vaccines were

or are still prepared with cells of kidney origin such as fetal bovine kidney cells, Vero cells (African green monkey cells), and, for experimental or veterinary uses, baby hamster kidney cells (BHK-21). All these cells, as can be predicted from the organ origin, are indeed highly positive for NCAM. In contrast, most fibroblast cell lines are NCAM negative and resistant to
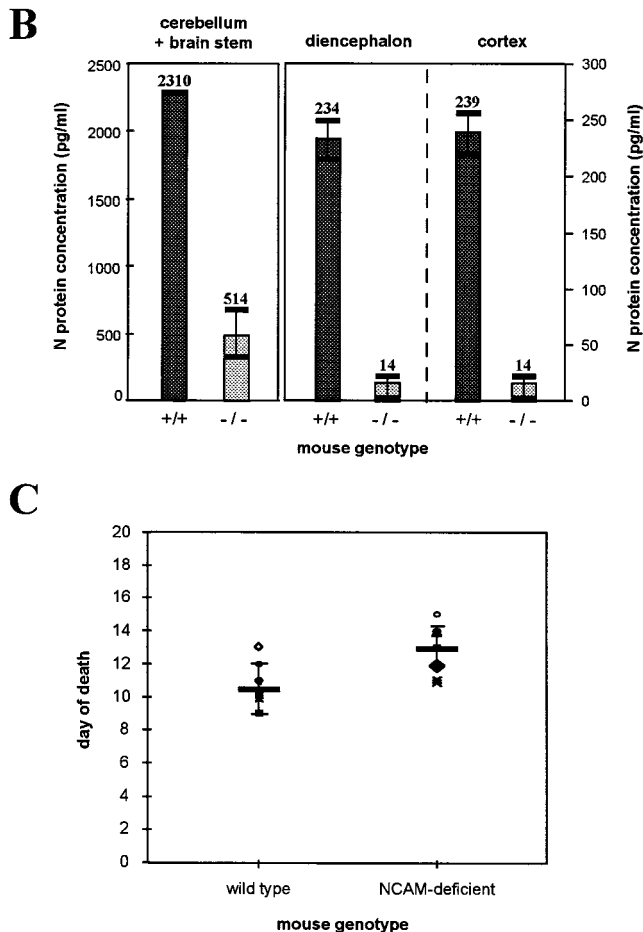
FIG. 7—Continued.

synapses (29). The fact that RV preferentially infects cells which express NCAM at a high density strongly suggests that a particular spatial organization of the receptors, in which each isoform could play a role, contributes to susceptibility to RV.

The heparan sulfate binding site has been located in the first and second Ig-like domains of NCAM (18) and mapped to a 25-kDa NH2-terminal fragment of NCAM and to the 17-amino-acid-long region of the second Ig-like domain (5, 6). The capacity of heparan sulfate to block RV infection suggests that the virus binding site is located in the first two Ig-like domains of NCAM. This conclusion need to be confirmed, for example, by mapping experiments to rule out the possibility that heparan sulfate binding has a steric occupancy effect or causes conformational changes in NCAM (8). Possibly, identification of the RV binding site in the first two Ig-like domains may help to elucidate the mechanisms by which RV induces neuronal dysfunction. NCAM is not only involved in cell recognition but is also capable of transducing recognition events. In particular, it has been shown that the stimulation of Ig-like I and/or II domains induces intracellular changes of inositol phosphate metabolim, Ca^{2+} flux, and pH (3, 23, 36). The binding of RV to a receptor that is also a signaling molecule may modify the metabolism of the neuronal cell target. This may contribute to neuronal perturbations or the behavioral changes that characterize rabies.

The membranes of hamster kidney cells, BHK-21 cells, contain a protein complex which is a receptor for RV but which has not yet been identified (33). This receptor was described as an RV-specific entity that functions independently of Ca^{2+} and Mg^{2+}. It consists of a doublet of high-molecular-weight protein and of at least four other proteins migrating between 66 and 200 kDa (4). The high-molecular-weight protein carrying the specific binding activity was described as an integral glycosylated membrane component and as being sensitive to pronase and subtilisin enzymatic treatment. We assessed whether NCAM does not belong to this complex receptor. We found that BHK-21 cells express NCAM. Moreover, both major isoforms of NCAM (-140 and -180) are glycosylated integral membrane proteins and are sensitive to pronase and subtilisin. NCAM binding activity does not require Ca^{2+} or Mg^{2+}. The properties shared by NCAM and the BHK-21 receptor, as well as the evidence that BHK-21 cells and their derived clone, BSR cells, use an NCAM-dependent pathway for RV infection, suggest that a glycosylated NCAM isoform is the main or even the only component of the BHK-21 receptor. However, the NCAM pathway is not the only mediator of RV penetration into kidney cells: RV infection can develop even in the o-called resistant cell lines (10% compared to 80 to 100% in NCAM-positive cells). This alternative route of entry was not inhibited by heparan sulfate or by preincubation with an anti-NCAM Ab. The nature of the NCAM-independent pathway used by the RV to infect kidney cells is unknown, but the pathway may involve a nonprotein receptor (4). Our data suggest, however, that this pathway is sensitive to chondroitin sulfate C treatment.

There is strong evidence that nicotinic AchR, especially α-bungarotoxin-sensitive nicotinic AchR at the muscular junction, can be used by the virus as a receptor. It is difficult to assess the respective roles of NCAM and AchR, as receptor analysis has been performed in cells or tissues expressing both NCAM and AchR, such as N2a cells (33), IMR-32 cells (22), myotubes, mouse diaphragm cells, and neuromuscular junctions (14). In blocking experiments, NCAM ligands were as efficient, or even more efficient, in N2a cells expressing both NCAM and AchR as, or than, in BSR cells expressing NCAM only. If AchR is functionally active in N2a cells, this indicates

RV infection. NIH 3T3 cells are an exception and can be infected by RV. This is probably due to their embryonic origin and the expression of the NCAM-140 isoform (34). The recent observations that macrophage-like lines (32) and lymphocytes (37), such as the mouse Wehi-7 cells, are susceptible to RV are consistent with CD56 antigen expression and the origin of these cells.

We found that a soluble NCAM preparation (a protein composed of the five Ig-like domains and the two fibronectin domains) blocked RV infection. This suggests that the RV G protein binding site is located in the NCAM ectodomain. We showed that BSR or NIH 3T3 cells expressing only the NCAM-140 isoforms, differentiated PC12 cells expressing only NCAM-180, and cells transfected with either genes encoding isoform 140 or genes encoding isoform 180 were susceptible to RV infection. This indicates that both NCAM isoforms, -140 and -180, which contain almost identical ectodomains, have similar receptor properties. Nevertheless, it can be envisaged that association or stabilization of one isoform by the other could result in a more efficient RV uptake: we showed that RV infects N2a cells more efficiently than NCAM-transfected cells. This may be due to the presence of three different NCAM isoforms in the N2a cells. The flexibility of the two isoforms is different: NCAM-180 has been reported to be less mobile than the -140 isoform because of its association with spectrin (30). The NCAM-180 isoform is found at high density at sites of cell-cell contact where it may be involved in stabilization of

that there may be functional synergy or a close-contact relationship between the two molecules. However, evidence is accumulating that NCAM and AchR function independently both in vitro and in vivo. First, the capacity of RV to infect NCAM-transfected cells lacking AchR clearly demonstrates that NCAM allows RV entry independently of AchR. In vivo, RV infects cells that are AchR negative such as microglia, Schwann cells, and spindle cells and reaches the nervous system after inoculation into sites lacking AchR such as the footpad or the anterior chamber of the eye or by intranasal instillation. These different sites, especially the olfactory bulb (25), express high levels of NCAM, consistent with NCAM playing a major role in vivo. Nevertheless, RV can reach the nervous system by routes lacking NCAM. Indeed, in NCAM-deficient mice some parts of the brain remain susceptible to RV infection despite the total lack of NCAM. These parts of the brain, which include the hippocampus and cerebellar Purkinje cells, bear α-bungarotoxin binding sites (24), suggesting that in NCAM-deficient mice the residual infection results from the AchR pathway. Thus, we propose that, like many other viruses and human immunodeficiency virus (38), RV may use more than one receptor to gain entry into the cell both in vitro and in vivo.

ACKNOWLEDGMENTS

REFERENCES

1. **Alcaraz, G., and C. Goridis.** 1991. Biosynthesis and processing of polysialylated NCAM by AtT-20 cells. Eur. J. Cell Biol. **55:**165–173.
2. **Atkinson, J. P., M. Krych, M. Nickells, D. Birmingham, V. B. Subramanian, L. Clemenza, J. Alvarez, and K. Liszewski.** 1994. Complement receptors and regulatory proteins: immune adherence revisited and abuse by microorganisms. Clin. Exp. Immunol. **2:**1–3.
3. **Beggs, H. E., S. C. Baragona, J. J. Hemperly, and P. F. Maness.** 1997. NCAM140 interacts with the focal adhesion kinase p125(fak) and the SRC-related tyrosine kinase p59(fyn). J. Biol. Chem. **272:**8310–8319.
4. **Broughan, J. H., and W. H. Wunner.** 1995. Characterization of protein involvement in rabies virus binding to BHK-21 cells. Arch. Virol. **140:**75–93.
5. **Cole, G. J., and R. Akeson.** 1989. Identification of a heparin binding domain of the neural cell adhesion molecule N-CAM using synthetic peptides. Neuron **2:**1157–1165.
6. **Cole, G. J., and L. Glaser.** 1986. A heparin-binding domain from N-CAM is involved in neural cell-substratum adhesion. J. Cell Biol. **102:**403–412.
7. **Cole, G. J., A. Loewy, and L. Glaser.** 1986. Neuronal cell-cell adhesion depends on interactions of N-CAM with heparin-like molecules. Nature **320:**445–447.
8. **Cole, G. J., D. Schubert, and L. Glaser.** 1985. Cell-substratum adhesion in chick neural retina depends upon protein-heparan sulfate interactions. J. Cell Biol. **100:**1192–1199.
9. **Cremer, H., R. Lange, A. Christoph, M. Plomann, G. Vopper, J. Roes, R. Brown, S. Baldwin, P. Kraemer, S. Scheff, et al.** 1994. Inactivation of the N-CAM gene in mice results in size reduction of the olfactory bulb and deficits in spatial learning. Nature **367:**455–459.
10. **Doherty, P., D. A. Mann, and F. S. Walsh.** 1988. Comparison of the effects of NGF, activators of protein kinase C, and a calcium ionophore on the expression of Thy-1 and N-CAM in PC12 cell cultures. J. Cell Biol. **107:**333–340.
11. **Frei, T., F. von Bohlen und Halbach, W. Wille, and M. Schachner.** 1992. Different extracellular domains of the neural cell adhesion molecule (N-CAM) are involved in different functions. J. Cell Biol. **118:**177–194.
12. **Gastka, M., J. Horvath, and T. L. Lentz.** 1996. Rabies virus binding to the nicotinic acetylcholine receptor alpha subunit demonstrated by virus overlay protein binding assay. J. Gen. Virol. **77:**2437–2440.
13. **Goridis, C., and J. F. Brunet.** 1992. NCAM: structural diversity, function and regulation of expression. Semin. Cell Biol. **3:**189–197.
14. **Hall, Z. W., and J. R. Sanes.** 1993. Synaptic structure and development: the neuromuscular junction. Cell **72:**99–121.
15. **Hartmann, U., C. Vens, G. Vopper, W. Wille, and U. A. Heinlein.** 1994. Ectopic expression of NCAM in mouse fibroblasts stimulates self-aggregation, and promotes integration into primary cerebellum cell aggregates. Cell Adhesion Commun. **2:**287–298.
16. **Hirn, M., M. Pierres, H. Deagostini-Bazin, M. R. Hirsch, C. Goridis, M. S. Ghandour, O. K. Langley, and G. Gombos.** 1982. A new brain cell surface glycoprotein identified by monoclonal antibody. Neuroscience **7:**239–250.
17. **Horuk, R., A. Martin, J. Hesselgesser, T. Hadley, Z. H. Lu, Z. X. Wang, and S. C. Peiper.** 1996. The Duffy antigen receptor for chemokines: structural analysis and expression in the brain. J. Leukocyte Biol. **59:**29–38.
18. **Kiselyov, V. V., V. Berezin, T. E. Maar, V. Soroka, K. Edvardsen, A. Schousboe, and E. Bock.** 1997. The first immunoglobulin-like neural cell adhesion molecule (NCAM) domain is involved in double-reciprocal interaction with the second immunoglobulin-like NCAM domain and in heparin binding. J. Biol. Chem. **272:**10125–10134.
19. **Lafon, M., and M. Lafage.** 1987. Antiviral activity of monoclonal antibodies specific for the internal proteins N and NS of rabies virus. J. Gen. Virol. **68:**3113–3123.
20. **Lanier, L. L., R. Testi, J. Bindl, and J. H. Phillips.** 1989. Identity of Leu-19 (CD56) leukocyte differentiation antigen and neural cell adhesion molecule. J. Exp. Med. **169:**2233–2238.
21. **Lentz, T. L., T. G. Burrage, A. L. Smith, and G. H. Tignor.** 1983. The acetylcholine receptor as a cellular receptor for rabies virus. Yale J. Biol. Med. **56:**315–322.
22. **Lentz, T. L., Y. Fu, and P. Lewis.** 1997. Rabies virus infection of IMR-32 human neuroblastoma cells and effect of neurochemical and other agents. Antiviral Res. **35:**29–39.
23. **Maness, P. F., H. E. Beggs, S. G. Klinz, and W. R. Morse.** 1996. Selective neural cell adhesion molecule signaling by Src family tyrosine kinases and tyrosine phosphatases. Perspect. Dev. Neurobiol. **4:**169–181.
24. **Marks, M. J., J. R. Pauly, E. U. Grun, and A. C. Collins.** 1996. ST/b and DBA/2 mice differ in brain alpha-bungarotoxin binding and alpha 7 nicotinic receptor subunit mRNA levels: a quantitative autoradiographic analysis. Mol. Brain Res. **39:**207–222.
25. **Miragall, F., G. Kadmon, M. Husmann, and M. Schachner.** 1988. Expression of cell adhesion molecules in the olfactory system of the adult mouse: presence of the embryonic form of N-CAM. Dev. Biol. **129:**516–531.
26. **Montano-Hirose, J. A., M. Lafage, and M. Lafon.** 1995. Measurement of rabies virus N protein in rabies vaccines. Res. Virol. **146:**217–224.
27. **Nieke, J., and M. Schachner.** 1985. Expression of the neural cell adhesion molecules L1 and N-CAM and their common carbohydrate epitope L2/HNK-1 during development and after transection of the mouse sciatic nerve. Differentiation **30:**141–151.
28. **Norkin, L. C.** 1995. Virus receptors: implications for pathogenesis and the design of antiviral agents. Clin. Microbiol. Rev. **8:**293–315.
29. **Pollerberg, E. G., R. Sadoul, C. Goridis, and M. Schachner.** 1985. Selective expression of the 180-kD component of the neural cell adhesion molecule N-CAM during development. J. Cell Biol. **101:**1921–1929.
30. **Pollerberg, E. G., M. Schachner, and J. Davoust.** 1986. Differentiation state-dependent surface mobilities of two forms of the neural cell adhesion molecule. Nature **324:**462–465.
31. **Prediger, E. A., S. Hoffman, G. M. Edelman, and B. A. Cunningham.** 1988. Four exons encode a 93-base-pair insert in three neural cell adhesion molecule mRNAs specific for chicken heart and skeletal muscle. Proc. Natl. Acad. Sci. USA **85:**9616–9620.
32. **Ray, N. B., L. C. Ewalt, and D. L. Lodmell.** 1995. Rabies virus replication in primary murine bone marrow macrophages and in human and murine macrophage-like cell lines: implications for viral persistence. J. Virol. **69:**764–772.
33. **Reagan, K. J., and W. H. Wunner.** 1985. Rabies virus interaction with various cell lines is independent of the acetylcholine receptor. Arch. Virol. **84:**277–282.
34. **Roubin, R., H. Deagostini-Bazin, M. R. Hirsch, and C. Goridis.** 1990. Modulation of NCAM expression by transforming growth factor-beta, serum, and autocrine factors. J. Cell Biol. **111:**673–684.
35. **Santoni, M. J., D. Barthels, G. Vopper, A. Boned, C. Goridis, and W. Wille.** 1989. Differential exon usage involving an unusual splicing mechanism generates at least eight types of NCAM cDNA in mouse brain. EMBO J. **8:**385–392.
36. **Schuch, U., M. J. Lohse, and M. Schachner.** 1989. Neural cell adhesion molecules influence second messenger systems. Neuron **3:**13–20.
37. **Thoulouze, M. I., M. Lafage, J. A. Montano-Hirose, and M. Lafon.** 1997. Rabies virus infects mouse and human lymphocytes and induces apoptosis. J. Virol. **71:**7372–7380.
38. **Tufaro, F.** 1997. Virus entry: two receptors are better than one. Trends Microbiol. **5:**257–258.
39. **Wunner, W. H., K. J. Reagan, and H. Koprowski.** 1984. Characterization of saturable binding sites for rabies virus. J. Virol. **50:**691–697.